Thin Solid Films 518 (2010) 1925–1928

Contents lists available at ScienceDirect

Thin Solid Films

journal homepage: www.elsevier.com/locate/tsf

Band alignment of $Cd_{(1-x)}Zn_xS$ produced by spray pyrolysis method

M. Celalettin Baykul *, Nilgun Orhan

Eskişehir Osmangazi University, Physics Department, 26480, Eskişehir, Turkey

ARTICLE INFO

Article history:
Received 5 January 2007
Received in revised form 9 July 2009
Accepted 17 July 2009
Available online 25 July 2009

Keywords:
$Cd_{(1-x)}Zn_xS$ thin films
Atomic force microscopy
X-ray diffraction
Band gap
Exciton binding energy

ABSTRACT

$Cd_{(1-x)}Zn_xS$ thin films have been grown on glass substrates by the spray pyrolysis method using $CdCl_2$ (0.05 M), $ZnCl_2$ (0.05 M) and H_2NCSNH_2 (0.05 M) solutions and a substrate temperature of 260 °C. The energy band gap, which depends on the mole fraction × in the spray solution used for preparing the $Cd_{(1-x)}Zn_xS$ thin films, was determined. The energy band gaps of CdS and ZnS were determined from absorbance measurements in the visible range as 2.445 eV and 3.75 eV, respectively, using Tauc theory. On the other hand, the values calculated using Elliott-Toyozawa theory were 2.486 eV and 3.87 eV, respectively. The exciton binding energies of $Cd_{0.8}Zn_{0.2}S$ and ZnS determined using Elliott-Toyozawa theory were 38 meV and 40 meV, respectively. X-ray diffraction results showed that the $Cd_{(1-x)}Zn_xS$ thin films formed were polycrystalline with hexagonal grain structure. Atomic force microscopy studies showed that the surface roughness of the $Cd_{(1-x)}Zn_xS$ thin films was about 50 nm. Grain sizes of the $Cd_{(1-x)}Zn_xS$ thin films varied between 100 and 760 nm.

1. Introduction

The production of thin films with tailored optical properties is an important challenge for research in optoelectronic applications [1]. Cadmium zinc sulphide ($Cd_xZn_{(1-x)}S$) thin films have received great attention due to their various optoelectronic applications. They have been used as a wide-band-gap window material for heterojunction solar cells [2,3], and the short wavelength optoelectronic devices such as II–VI semiconductor laser diodes, ZnSe/CdZnSe lasing at ~500 nm. In order to have true blue, violet, or even ultraviolet laser diodes, and to have better optical and carrier confinements, higher band gap materials are needed [4–6]. The optical properties of alloy semiconductor films can be varied by changing their composition and this can be exploited. In particular, $Cd_{(1-x)}Zn_xS$ thin films possess energy gaps higher than the band gap of a CdS thin film (E_g ~2.4 eV) [7,8], while $Cd_{(1-x)}Zn_xS$ thin films possess band gaps (E_g<3.5 eV) narrower than the energy gap (E_g ~3.7 eV) of ZnS thin film [9,10]. $Cd_xZn_{(1-x)}S$ can be assumed to be an ideal alternative material since its composition can be simply controlled.

Most II–VI semiconductor compounds are direct-band-gap materials [11]. The band gaps of CdS with hexagonal structure and the lattice parameters $a=4.136$ Å and $c=6.714$ Å are 2.573 eV and 2.485 eV at the temperatures 80 K and 293 K, respectively, while the energy gap of CdS with cubic structure and the lattice parameter $a=5.825$ Å is 2.5 eV. On the other hand, the energy gap of ZnS with cubic structure and the lattice parameter $a=5.410$ Å is 3.78 eV at 19 K, while the energy gap of hexagonally structured ZnS with the lattice parameters $a=3.822$ Å and $c=6.260$ Å is 3.74 eV [12]. The energy band gaps of CdS thin films produced using different techniques vary between 2.26 and 2.50 eV, while the band gaps of ZnS thin films vary between 3.5 and 3.8 eV [7,13–15]. The energy band gap of a $Cd_{(1-x)}Zn_xS$ thin film can be determined by UV–Vis spectrometry.

The exciton binding energy serves as a critical criterion for identifying the nature of elementary excitations in semiconductor materials [16]. Excitons are also a sensitive indicator of the material quality [17]. The energy band gap E_g and the exciton binding energy E_x of $Cd_{(1-x)}Zn_xS$ thin films can be determined via the Elliott–Toyozawa [18,19] theory, which describes the optical absorption as being due to the formation of excitons [11,20]. Analysis of the absorption spectra within the Elliott–Toyozawa theory frame, allows for the determination of the energy gap, the exciton binding energies, the valence band splitting, and the radiative constant.[Float1] The absorption coefficient derived from the Elliott–Toyozawa theory is given by

$$\alpha(E)=\sum_i \frac{\alpha_i}{1+[(E-E_i)/\Gamma_i]^2}+\frac{\alpha_\infty}{1+exp\left[-\left(E-E_g\right)/kT\right]}\frac{exp\left(R_y^*\pi^2/|E-E_g|\right)^{\frac{1}{2}}}{Sinh\left(R_y^*\pi^2/|E-E_g|\right)^{\frac{1}{2}}} \quad (1)$$

where α_i and α_∞ are the absorption coefficients of the 1 s exciton and the continuum states, respectively, while R_y^* and Γ_i are the 1 s exciton

* Corresponding author.
E-mail address: cbaykul@ogu.edu.tr (M.C. Baykul).

0040-6090/$ – see front matter © 2009 Elsevier B.V. All rights reserved.
doi:10.1016/j.tsf.2009.07.142

binding energy and the width of the exciton density of states, respectively [21].

CdZnS thin films have been produced by metal–organic vapour phase epitaxy and molecular beam epitaxy, vacuum evaporation, spray pyrolysis, radio-frequency sputtering, solution growth, sublimation growth, and the screen-printing method [4,22]. The spray pyrolysis method is an economical and easy technique for the production of II–VI compound semiconductors [22].

This paper reports the band alignment of $Cd_{(1-x)}Zn_xS$ thin films produced by the spray pyrolysis method and their characterization by X-ray diffraction (XRD) and atomic force microscopy (AFM). The energy band gap and the exciton binding energy were also determined by the Elliott–Toyozawa theory. The spray pyrolysis can be an alternative technique for the preparation of II–VI thin films suitable for electronic devices, high-efficiency solar cells and the light emitter applications.

2. Experimental details

$Cd_{(1-x)}Zn_xS$ thin films were produced on a glass substrate by the spray pyrolysis technique. The $ZnCl_2$, $CdCl_2$ salts and H_2NCSNH_2 were dissolved in deionized water in separate beakers. Aqueous solutions of $ZnCl_2$, $CdCl_2$, and H_2NCSNH_2 were used as the sources of Zn, Cd, and S, respectively. The $ZnCl_2$, $CdCl_2$ and H_2NCSNH_2 solutions were mixed for 30 min. with a magnetic stirrer. The compositions of the solutions used to fabricate the $Cd_{(1-x)}Zn_xS$ thin films are shown in Table 1 in terms of the nominal concentrations in the deposition solution. The substrate temperature was regulated at 260 ± 6 °C during the deposition process using a resistive heater and a thermocouple. Glass substrates were prepared by cutting $10 \times 10 \times 1$ mm^3 pieces from the microscope slides produced by ISOLAB Laborgeräte GmbH and they were placed on a copper block with the same dimension. In order to spray the solution onto the substrate using an ultrasonic atomizer, nitrogen (N_2) was used as the carrier gas at a pressure of 10^5 Pa with a deposition rate of 5 cm^3/min during the deposition process. At the end of the spraying process, nitrogen (N_2) was flowed onto the thin films formed on the glass substrate for 5 min in order to dry them. They were then cooled down naturally to room temperature [22].

The thickness of the $Cd_{(1-x)}Zn_xS$ thin films was measured using the eddy-current technique with an Elcometer 345 coating thickness gauge. Structural characterization of the $Cd_{(1-x)}Zn_xS$ thin films was carried out by XRD (Rigaku RINT 2000 spectrometer) using Cu kα radiation in the Bragg-Brentano configuration. The optical absorption spectra of the $Cd_{(1-x)}Zn_xS$ thin films were obtained in the wavelength range 300 to 600 nm using a Perkin-Elmer Lambda 2 UV-Vis double-beam spectrometer. Morphological characterization of the films was performed by AFM (Nanomagnetics instruments) in non-contact mode under ambient pressure and temperature. For the non-contact AFM studies, a 30 nm thick aluminium reflex coated Tap300Al AFM cantilever (Budget Sensors) with a resonance frequency of 300 kHz was used. The spring constant of the cantilever was 40 N/m. The dimensions of the cantilever were $125 \times 30 \times 4$ μm^3 and the tip height was 17 μm.

Table 1
Solutions used for the production of $Cd_{(1-x)}Zn_xS$ thin films.

Nominal Composition of $Cd_{(1-x)}Zn_xS$ (x)	$CdCl_2$ (0.05 M) (ml)	$ZnCl_2$ (0.05 M) (ml)	H_2NCSNH_2 (0.05 M) (ml)
0.0	100	–	100
0.2	100	25	125
0.4	60	40	100
0.6	40	60	100
0.8	20	80	100
1.0	–	100	100

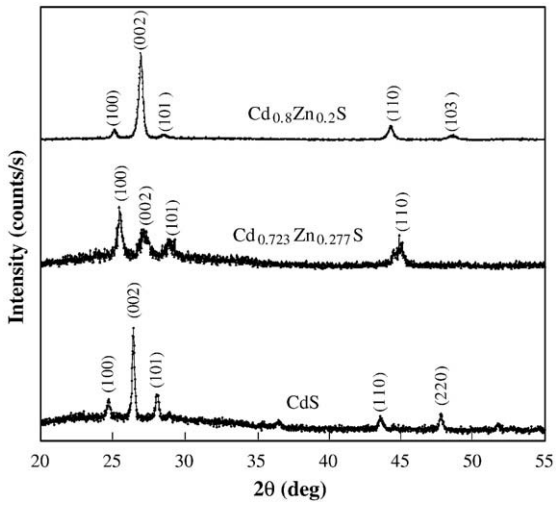

Fig. 1. XRD pattern of thin films with the nominal compositions CdS, $Cd_{0.723}Zn_{0.277}S$, and $Cd_{0.8}Zn_{0.2}S$ produced at 260 °C. The films are indexed based on the JCPDS cards # 041-1049, 040-0836, and 040-0835, respectively [23].

3. Results and discussion

3.1. Structural properties of $Cd_{(1-x)}Zn_xS$

The XRD patterns of the CdS, $Cd_{0.6}Zn_{0.4}S$ and $Cd_{0.8}Zn_{0.2}S$ thin-film samples are shown in Fig. 1. For the CdS thin film, the (100), (002), (101) and (110) diffractions are related to hexagonal CdS, while the (220) diffraction is related to cubic CdS. The preferred crystallographic orientation of the CdS thin film is (0002). For the $Cd_{0.6}Zn_{0.4}S$ thin film, the (100), (002), (101) and (110) diffractions are related to a hexagonal $Cd_{0.723}Zn_{0.277}S$ thin film, as shown in Fig. 1. Actually, the process was designed to fabricate a $Cd_{0.6}Zn_{0.4}S$ thin film, but instead a $Cd_{0.723}Zn_{0.277}S$ thin film was produced. The XRD pattern of the $Cd_{0.8}Zn_{0.2}S$ thin film shows (100), (002), (101), (110) and (103) diffractions. The preferred crystallographic orientation of the $Cd_{0.8}Zn_{0.2}S$ thin film is (0002). The thickness of the $Cd_{(1-x)}Zn_xS$ thin films was about 1 μm.

3.2. Optical properties of $Cd_{(1-x)}Zn_xS$ thin films

The optical absorption spectra of $Cd_{(1-x)}Zn_xS$ thin films were obtained in the wavelength range 300 to 600 nm. The optical absorbance was measured from these spectra. According to Tauc, the dependence of the absorption coefficient α on the photon energy $h\nu$ for near- edge optical absorption in semiconductors takes the form

$$(\alpha h\nu)^{1/m} = k\left(h\nu - E_g\right) \tag{2}$$

where E_g is the optical band gap, k is a constant and $m = 1/2$ for an allowed direct energy gap and $m = 3/2$ for a forbidden direct energy gap [22,24]. In order to determine the optical band gap of the $Cd_{(1-x)}Zn_xS$ thin film, taking $m = 1/2$, $(\alpha h\nu)^2$ was plotted versus $h\nu$ using the data obtained from the optical absorption spectra. The direct band gap of the $Cd_{(1-x)}Zn_xS$ thin film was obtained by extrapolating the linear part to the zero of the ordinate [25]. A typical plot of $(\alpha h\nu)^2$ versus $h\nu$ for the $Cd_{0.8}Zn_{0.2}S$ thin film is shown in Fig. 2. The band gap of the $Cd_{0.8}Zn_{0.2}S$ film was estimated to be 2.61 eV.

The calculations of the absorption coefficients based on the theory of Elliott and Toyozawa for $Cd_{(1-x)}Zn_xS$ ($x = 0.0$, 0.2, 0.4, 0.6, and 1.0) thin films have been fitted with the measured data of the optical absorption spectra. A typical fit for $Cd_{0.8}Zn_{0.2}S$ is shown in Fig. 3. The parameters used to fit the $Cd_{0.8}Zn_{0.2}S$ thin film were $\alpha_i = 2.0 \times 10^4$ cm^{-1}, $\alpha_\infty = 5.08 \times 10^4$ cm^{-1}, $R_y^* = 0.026$ eV, $\Gamma_i = 1.4$ eV, $E_i = 2.62$ eV (the energy of the exciton state), $E_g = 2.658$ eV, and $kT = 0.047$ eV. The best-

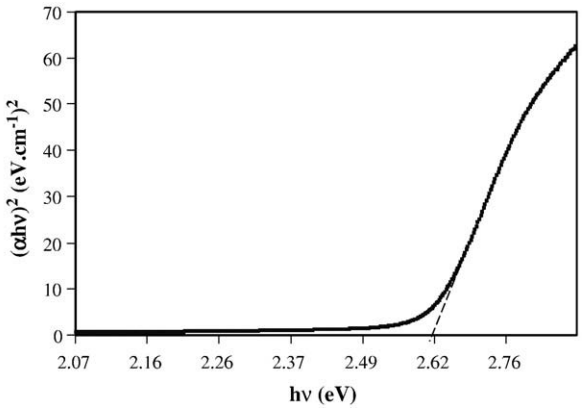

Fig. 2. Plot of $(\alpha h\nu)^2$ vs. $h\nu$ for the $Cd_{0.8}Zn_{0.2}S$ thin film.

fit values for the energy band gap and the exciton binding energy of the $Cd_{(1-x)}Zn_xS$ samples are shown in Table 2.

The relationship between the energy band gaps of the $Cd_{(1-x)}Zn_xS$ thin films and the Zn content (x) has been determined using a quadratic model for fitting the $E_g(x)$ values given in Table 2 as

$$E_g(x) = E_g(CdS) + \left(E_g(ZnS) - E_g(CdS) - 0.658\right)x + 0.658x^2 \text{ for} (0<x<1). \quad (3)$$

where $E_g(CdS) = 2.445$ eV and $E_g(ZnS) = 3.75$ eV are the energy band gaps of CdS and ZnS thin films, respectively. Fig. 4 shows the plot of the energy gaps of $Cd_{(1-x)}Zn_xS$ versus the zinc content (x).

3.3. Surface morphology of $Cd_{(1-x)}Zn_xS$ thin films

The morphological characteristics of $Cd_{(1-x)}Zn_xS$ thin films were determined by AFM in contact mode. 2 μm × 2 μm areas of the surfaces of $Cd_{(1-x)}Zn_xS$ thin films were imaged. A typical AFM topographic image of a ZnS thin film is shown in Fig. 5(a). Fig. 5(b, c, d) show AFM images of $Cd_{0.8}Zn_{0.2}S$, $Cd_{0.6}Zn_{0.4}S$ and CdS thin films. The AFM image of ZnS (Fig. 5(a)) shows that the grain size varies between 350 and 760 nm and the surface roughness is about 45 nm. The sizes of individual grains and the surface roughness of the $Cd_{0.8}Zn_{0.2}S$ thin film vary between 250 and 500 nm and 60 nm, respectively, as shown in Fig. 5(b). The AFM image of the $Cd_{0.6}Zn_{0.4}S$ thin film is shown in Fig. 5(c). The sizes of individual grains and the surface roughness of the film are between 100 and 250 nm and about 15 nm, respectively. The sizes of individual grains of the CdS thin film are between 400 and 1250 nm and the surface roughness of that sample is determined as 180 nm (Fig. 5(d)). By means of the spray pyrolysis method, $Cd_{(1-x)}Zn_xS$ thin films have been obtained in desired surface roughnesses and grain sizes.

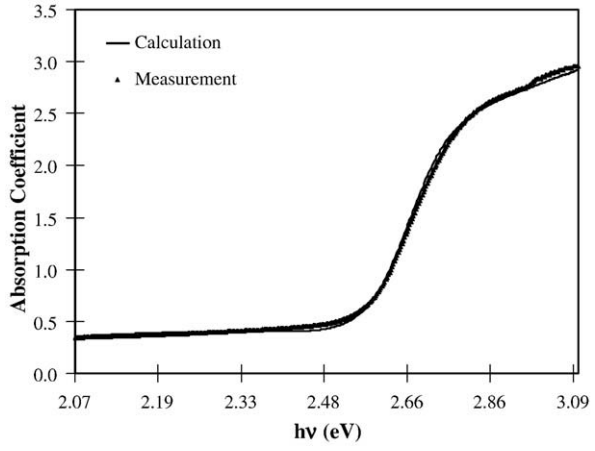

Fig. 3. Optical absorption spectra of the $Cd_{0.8}Zn_{0.2}S$ thin film in the energy range 2.07 eV to 3.11 eV. Dashed line is the best-fit curve calculated with the theory of Elliott and Toyozawa.

Table 2
Energy band gaps and the exciton binding energies of $Cd_{(1-x)}Zn_xS$ thin films.

Composition (x)	Band gap (eV) (±0.004 eV) (Tauc Method)	Band gap (eV) (±0.002 eV) (Elliott-Toyozawa Method)	Exciton binding energy (meV)
0.0	2.445	2.486	–
0.2	2.610	2.658	38
0.4	2.830	2.830	40
0.6	3.070	3.080	20
0.8	3.220	3.279	–
1.0	3.750	3.870	40

4. Conclusions

We have shown that $Cd_{(1-x)}Zn_xS$ thin films can be formed on glass substrates by spray pyrolysis. The films were characterized by XRD, AFM and optical absorption spectroscopy. Energy band gaps of the $Cd_{(1-x)}Zn_xS$ samples obtained using optical absorption spectra vary between 2.445 and 3.75 eV, while the band gaps obtained using a theoretical fit with the Elliott–Toyozawa theory vary between 2.486 and 3.87 eV. Furthermore, the results of the Elliott and Toyozawa theory for the calculation of the energy band gaps of $Cd_{(1-x)}Zn_xS$ thin films are in agreement with those from the Tauc theory. The energy band gap of $Cd_{(1-x)}Zn_xS$ thin films increases quadratically with increasing zinc content. The exciton binding energies of $Cd_{(1-x)}Zn_xS$ thin films were determined as ~40 meV [26–28], in agreement with other published exciton binding energies. It has been demonstrated that the optoelectronic properties of $Cd_{(1-x)}Zn_xS$ semiconductor alloys can be tailored. XRD results have shown that in the deposition conditions used, the $Cd_{(1-x)}Zn_xS$ thin films on glass substrates are in the polycrystalline form. The grains of these thin films have a hexagonal structure. The XRD pattern of the CdS thin film has shown that its preferred orientation is in the <0002> direction. However, a cubic structure also forms in the <220> direction.

$Cd_{0.8}Zn_{0.2}S$ and $Cd_{0.6}Zn_{0.4}S$ thin films are of hexagonal structure. The crystallite sizes observed by AFM of the $Cd_{(1-x)}Zn_xS$ thin films vary between 100 and 760 nm. The surface roughnesses of the $Cd_{(1-x)}Zn_xS$ thin films have been determined to vary between 15 and 60 nm. On the other hand, the surface roughness of the CdS thin film was 180 nm.

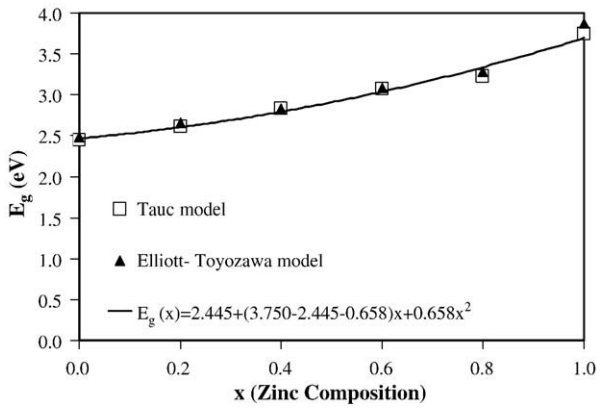

Fig. 4. Plot of energy gap of $Cd_{(1-x)}Zn_xS$ thin films versus zinc content x.

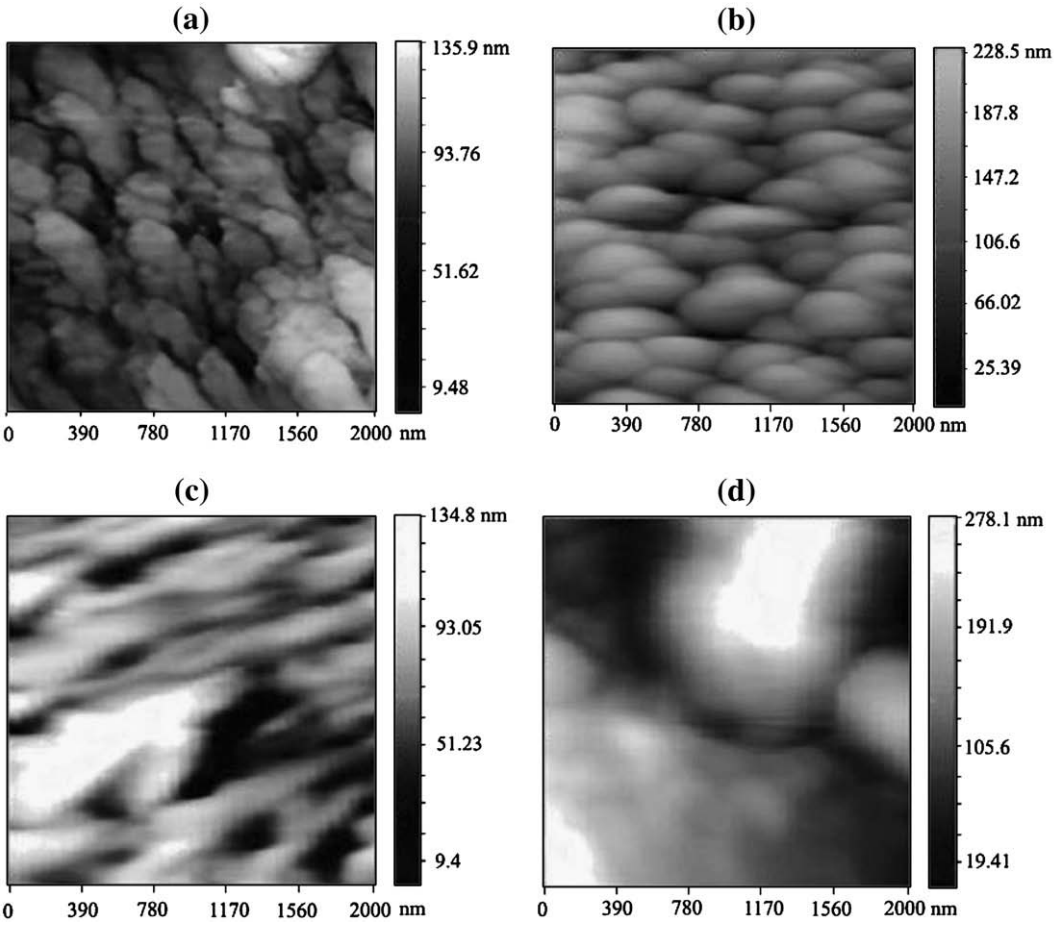

Fig. 5. AFM topographic images of the ZnS (a), $Cd_{0.8}Zn_{0.2}S$ (b), $Cd_{0.6}Zn_{0.4}S$ (c), and CdS (d) thin films. The scanned area of all samples is 2.0 μm × 2.0 μm.

Acknowledgments

The authors wish to thank A. Oral and F. Cansizoglu for providing the AFM images, H. Unluce for the XRD patterns, and A. Gulec for assistance with the experiments.

References

[1] N. Barreau, J.C. Bernède, S. Marsillac, A. Mokrani, J. Cryst. Growth 235 (2002) 439.
[2] O. Akinci, H.H. Gurel, H. Unlu, Thin Solid Films 511–512 (2006) 684.
[3] H. Zang, X. Ma, D. Yang, Mater. Lett. 58 (2003) 5.
[4] B.J. Wu, H. Cheng, S. Guha, M.A. Haase, J.M. De Puydt, G. Meis-Haugen, J. Qiu, Appl. Phys. Lett. 63 (1993) 2935.
[5] J.H. Lee, W.C. Song, K.J. Yang, Y.S. Yoo, Thin Solid Films 416 (2002) 184.
[6] M.A. Redwan, L.I. Soliman, E.H. Aly, A.A. El-Shazely, H.A. Zayed, J. Mater. Sci. 38 (2003) 3449.
[7] R.N. Bhattacharya, K. Ramanathan, Sol. Energy 77 (2004) 679.
[8] K.G.U. Wijayantha, L.M. Peter, L.C. Otley, Sol. Energy Mater. Sol. Cells 83 (2004) 363.
[9] J. Vidal, O. Vigil, O. de Melo, N. López, O. Zelaya-Angel, Mater. Chem. Phys. 61 (1999) 139.
[10] H.Y. Lu, S.Y. Chu, S.S. Tan, J. Cryst. Growth 269 (2004) 385.
[11] W.W. Chow, S.W. Koch, M. Sargent III, Semiconductor-Laser Physics, Springer, New York, 1997, p. 35.
[12] O. Madelung, Semiconductors-Basic Data, 2nd revised ed., Springer-Verlag, Berlin, 1996, pp. 182–185, Landolt-Börnstein Volumes.
[13] R. Zhai, S. Wang, H.Y. Xu, H. Wang, H. Yan, Mater. Lett. 59 (2005) 1497.
[14] M.B. Ortuño-López, M. Sotelo-Lerma, A. Mendoza-Galván, R. Ramírez-Bon, Thin Solid Films 457 (2004) 278.
[15] V. Kumar, V. Singh, S.K. Sharma, T.P. Sharma, Opt. Mater. 11 (1998) 29.
[16] Y.Z. Ma, L. Valkunas, S.M. Bachilo, G.R. Fleming, J. Phys. Chem. B 109 (2005) 15671.
[17] J.F. Muth, J.H. Lee, I.K. Shmagin, R.M. Kolbas, H.C. Casey Jr., B.P. Keller, U.K. Mishra, S.P. DenBaars, Appl. Phys. Lett. 71 (1997) 2572.
[18] R.J. Elliott, Phys. Rev. 108 (1957) 1384.
[19] Y. Toyozawa, Prog. Theor. Phys. 20 (1958) 53.
[20] M. Fernández, P. Prete, N. Lovergine, A.M. Mancini, R. Cingolani, L. Vasanelli, M.R. Perrone, Phys. Rev., B 55 (1997) 7660.
[21] S. Yano, R. Schroeder, B. Ullrich, H. Sakai, Thin Solid Films 423 (2003) 273.
[22] M.C. Baykul, A. Balcioglu, Microelectron. Eng. 51–52 (2000) 703.
[23] International Centre for Diffraction Data, JCPDS-PDF2 Data Base, Newtown Square, PA, 19073, 1998.
[24] Y.P. Chou, S.C. Lee, J. Appl. Phys. 83 (1998) 4111.
[25] S.S. Siddiqui, C.F. Desai, Thin Solid Films 239 (1994) 166.
[26] S. Adachi, Properties of Group-IV, III–V and II–VI Semiconductors, John Wiley & Sons Ltd, Chichester, 2005, p. 234.
[27] R. Memming, Semiconductor Electrochemistry, Wiley-VCH Verlag GmbH, Weinheim, 2001, p. 266.
[28] J. Puls, F. Henneberger, M. Rabe, A. Siarkos, J. Cryst. Growth 184/185 (1998) 787.